VBPCM: A Valence Bond Method that Incorporates a Polarizable Continuum Model

Lingchun Song,[†] Wei Wu,*[,†] Qianer Zhang,[†] and Sason Shaik[‡]

Department of Chemistry, Center for Theoretical Chemistry, and State Key Laboratory of Physical Chemistry of Solid Surfaces, Xiamen University, Xiamen, Fujian 361005, China, and Department of Organic Chemistry and the Lise Meitner-Minerva Center for Computational Quantum Chemistry, The Hebrew University, Jerusalem 91904, Israel

Received: February 5, 2004; In Final Form: May 10, 2004

The paper introduces a valence bond (VB) method that incorporates a polarizable continuum model of solvation, the self-consistent reaction field model. The solvation model achieves self-consistency for the charge density of the solute based on a linear combination of VB structures that interact with the reaction field of the solvent. The coupling of VB calculations with a solvent model enables one to compute the ab initio energy profiles of individual VB structures that contribute to a given state and to quantify the VB parameters of the VB state correlation diagram model in solution. Test calculations for a few systems show the validity of the method, which adds to the increasing capabilities of ab initio VB methodology.

Introduction

Solvation effects play a very important role in molecular energy, structures, and properties.[1−4] In the last two decades, the topic of solute−solvent interactions has occupied a central place in theoretical chemistry. In this sense, the simplest continuum solvation model has proven to be an efficient and economical tool for describing solvation problems.[5−9] In continuum methods, the solvent is usually represented as a homogeneous medium that is characterized by a single dielectric constant. The charge distribution of the solute induces polarization of the surrounding dielectric medium. The interaction between the solute charges and the polarized electric field of the solvent is taken into account through an interaction potential that is determined by a self-consistent reaction field (SCRF) procedure. In ab initio quantum chemistry packages, the state function is solved by embedding the interaction potential in the molecular Hamiltonian and solving self-consistently the Schrödinger equation. At present, various levels of ab initio molecular orbital (MO) methods, such as Hartree−Fock, MP2, MCSCF, etc., are implemented with solvent capabilities.

One of the key features of valence bond (VB) theory is that its wave function is expressed in terms of a linear combination of VB functions, which correspond to specific chemical structures. In this manner, the wave function offers a springboard for many fundamental concepts such as resonance, hybridization, covalency, ionicity, and so on. Thus, while MO-based theory is the dominant computational method in quantum chemistry, VB theory still remains a widespread conceptual matrix for chemists. The stumbling block for efficient developments in ab initio VB theory has always been the use of nonorthogonal orbitals, which lead to enormous computational effort. However, thanks to the rapid recent development of computers and computing science, VB theory has enjoyed a surge of methodology developments, which enables its application to a variety of chemical problems.[10] With these ongoing developments in VB methodology, it is time to attempt incorporating solvent effects into ab initio VB theory.

One of the first successes in incorporating solvation effects into a VB method was the empirical valence bond (EVB) method of Warshel and Weiss.[11a] In their study on proton transfer, the authors constructed Hamiltonian matrix elements by use of empirical parameters and solved the usual secular equations to obtain the states and their energies. This method has formed a basis for the treatment of enzymatic reactions in their native proteins.[11b] One of us (S.S.) used a number of properties related to the solvent (static and optical dielectric constants) and the solvent−reactant interactions (desolvation energies) to discuss solvent effects in S_N2 reactions and in other processes that involve nucleophile−electrophile recombinations.[12] Hynes and co-workers developed a method for calculating the electronic structure of a solute and its reaction pathways, in a manner that incorporates nonequilibrium and equilibrium solvation effects.[13] Recently, Amovilli et al. presented a method to carry out VB analysis of complete active space-self consistent field wave functions in aqueous solution.[14] Though Amovilli's approach provided the diabatic profiles for chemical reactions, these diabatic profiles are not variational and are not derived directly from VB calculations. Mo and Gao developed a hybrid MO-VB method that includes the effect of solvation.[15] In their work, the localized wave function is based on a single determinant and, hence, cannot provide the entire diabatic energy profiles. As part of our long-term goal to develop ab initio VB methods that incorporate solvation models, the present work describes a methodology that couples VB theory with a standard polarizable continuum method (PCM).[16] Even though this is only the first step, the paper shows clearly the advantages of this strategy that provides means to quantitate the solvent effect on both the diabatic and adiabatic profiles.

This paper is organized as follows: It starts with brief reviews of the necessary theory of the VB method and the PCM model. The combined approach of VBPCM approach is described in the next section. Subsequently, a few test calculations are performed, including the bond dissociation processes of LiF,

* To whom correspondence may be addressed. E-mail: weiwu@xmu.edu.cn. Fax: 86-592-2186207. Tel: 86-592-2182825.
[†] Xiamen University.
[‡] The Hebrew University.

10.1021/jp049467c CCC: $27.50
Published on Web 06/17/2004

CH_3F, and $(CH_3)_3CCl$ and the identity S_N2 reaction, $Cl^- + CH_3Cl \rightarrow ClCH_3 + Cl^-$.

Theory and Methodology

A. The Spin-Free Approach for Valence Bond Theory. Before discussing the coupling of VB and PCM, let us briefly outline the elements of the spin-free approach for VB theory.[17,18] In the spin-free VB theory, the many-electron wave function is expressed in terms of spin-free VB functions Φ_K

$$\Psi = \sum_K C_K \Phi_K \tag{1}$$

Φ_K may be a bonded tableau state,[18] defined as

$$\Phi_K = N_K e_{r1}^{[\lambda]} \Omega_K \tag{2}$$

where N_K is a normalization factor, $e_{rs}^{[\lambda]}$ is a standard projector of symmetric group S_N defined through the irreducible representation of the matrix elements, $D_{rs}^{[\lambda]}(P)$, as follows

$$e_{rs}^{[\lambda]} = \left(\frac{f_\lambda}{N!}\right)^{1/2} \sum_P D_{rs}^{[\lambda]}(P) P \tag{3}$$

Here f_λ is the dimension of the irreducible representation $[\lambda]$ and Ω_K is an orbital product, eq 4

$$\Omega_K = \phi_{k1}(1)\phi_{k2}(2)\phi_{k3}(3)\phi_{k4}(4)...\phi_{k_N}(N) \tag{4}$$

that maintains a one-to-one correspondence with the usual VB structure through the sequence of orbital indices.

Having this permutation symmetry-adapted basis in eq 2, the Hamiltonian and overlap matrix elements are written respectively as

$$H_{KL} = \langle \Phi_K | H | \Phi_L \rangle = \sum_{P \in S_N} D_{11}{}^{[\lambda]}(P) \langle \Omega_K | HP | \Omega_L \rangle \tag{5}$$

and

$$M_{KL} = \langle \Phi_K | \Phi_L \rangle = \sum_{P \in S_N} D_{11}{}^{[\lambda]}(P) \langle \Omega_K | P | \Omega_L \rangle \tag{6}$$

The coefficients C_K in eq 1 are subsequently determined by solving the usual secular equation $\mathbf{HC} = E\mathbf{MC}$.

The weights of the VB structures were determined by use of the Coulson−Chirgwin formula,[19] eq 7, which is the equivalent of a Mulliken population analysis in VB theory

$$W_K = C_K{}^2 + \sum_{L \neq K} C_K C_L \langle \Phi_K | \Phi_L \rangle \tag{7}$$

B. Solute−Solvent Interactions. *The PCM Model in MO-Based Calculations.* In the ab initio quantum mechanics (QM) packages of the PCM, the solute molecule is studied quantum mechanically and the interaction between solute and solvent is represented by an interaction potential, V_R, which is treated as a perturbation on the Hamiltonian of the solute molecule

$$H^0 \Psi^0 = E^0 \Psi^0 \tag{8}$$

$$(H^0 + V_R)\Psi = E\Psi \tag{9}$$

where H^0 is the Hamiltonian of the solute molecule in a vacuum, Ψ^0 and Ψ are the state wave functions of the solute in a vacuum and in solution, respectively, and E^0 and E are their corresponding respective energies. It is helpful to express the interaction potential as

$$V_R = V_R'(\Psi) + V_R'' \tag{10}$$

where the first term depends explicitly on the wave function of the solute, while the second term is independent of the wave function. It can be shown[20] that the solution of eq 9 is obtained by minimizing the following function, G

$$G = \left\langle \Psi \middle| H^0 + V_R'' + \frac{1}{2} V_R'(\Psi) \middle| \Psi \right\rangle \tag{11}$$

under the constraint condition $\langle \Psi | \Psi \rangle = 1$. The contribution to the interaction potential is usually classified as a sum of electrostatic, repulsion, and dispersion components, as in eq 12

$$V_R = V_{el} + V_{dis} + V_{rep} \tag{12}$$

In principle, the above three terms depend on the charge distribution of the solute. However, in the standard implementation, the treatment reduces the interaction potential to the electrostatic component in the QM calculation, while the contributions from the other terms are based on empirical parameters. Therefore, the total free energy can be written as in eq 13

$$G = \langle \Psi | H^0 | \Psi \rangle + \langle \Psi | V_R'' | \Psi \rangle + \frac{1}{2} \langle \Psi | V_R'(\Psi) | \Psi \rangle + V_{NN} + G_{nel} \tag{13}$$

where V_{NN} is nuclear repulsion energy and G_{nel} stands for the contributions from nonelectrostatic components. The factor $^1/_2$ of V_R' is required in order to account for the energy change in the solvent as a result of its polarization by the solute.

In the Hartree−Fock approximation, the minimization of the free-energy functional G, eq 13, is reduced to a Hartree−Fock equation

$$\mathbf{F}^S\mathbf{C} = \mathbf{SC}\boldsymbol{\varepsilon} \tag{14}$$

where the Fock matrix $\mathbf{F}^S$ is different from the one in a vacuum since it embeds the solvent related terms.

PCM in VB Calculations. To incorporate solvent effect into a VB scheme, the state wave function, Ψ, is expressed in the usual terms as a linear combination of VB structures, eq 1, but now, these VB structures are optimized and interact with one another in the presence of a polarizing field of the solvent. Thus, instead of solving eq 14 for Hartree−Fock method, the Schrödinger equation, eq 9, is solved directly by a self-consistent procedure. The interaction potential V_R for the ith iteration is given as a function of electronic density of the $(i-1)$th iteration and is expressed in the form of one-electronic matrix elements that are computed by a standard PCM procedure. The detailed procedures are as follows:

(1) A VB self-consistent (VBSCF)[21] procedure in a vacuum is performed, and the electron density is computed.

(2) Given the electron density from Step 1, effective one-electron integrals are obtained by a standard PCM subroutine.

(3) A standard VBSCF calculation is carried out with the effective one-electron integrals obtained from Step 2. The electron density is computed with the newly optimized VB wave function.

(4) Repeat steps 2 and 3 until the energy difference between the two iterations reaches a given threshold, which in the present paper is set at 10^{-6} hartree.

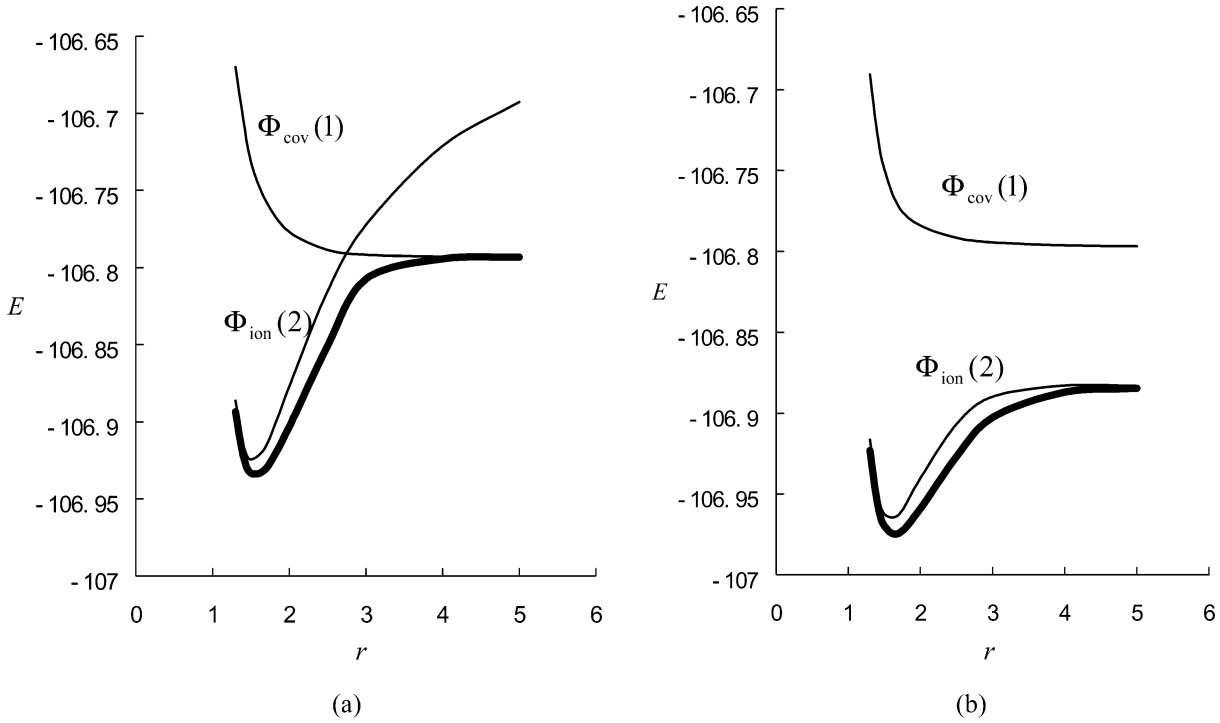

Figure 1. (a) VBSCF/6-31G* dissociation energy profiles of LiF in a vacuum. Adiabatic potentials are shown in bold curves. (b) VBPCM//VBSCF/6-31G* dissociation energy profiles of LiF in H_2O.

Having the optimized wave function, the final energy of system in solution is evaluated by eq 15

$$E = \left\langle \Psi \middle| H^0 + \frac{1}{2} V_R \middle| \Psi \right\rangle \tag{15}$$

As explained for eq 13, here too, the factor $^1/_2$ of V_R accounts also for the energy change in the solvent due to its polarization by the solute.

By performing the above procedures, the solvent effect is taken into account at the VBSCF level, whereby the orbitals and structural coefficients are optimized till self-consistency is achieved. This will be referred to hereafter as the VBPCM//VBSCF method, where the second indicator signifies the level of VB theory used in the procedure. The most straightforward implementation of the method is achieved by interfacing a standard VB package to a quantum chemistry package having a PCM facility. In the present paper, we use the GAMESS package (Version: 20 JUNE 2002 (R2))[22] for the PCM part of the calculation and the Xiamen VB (XMVB) package[23] for the VB calculation. An interface between the two codes is written to transfer to input/output files between the two codes. The integral equation formalism (IEF) PCM model[24] is chosen in the present paper. The cavity has been defined in terms of van der Waals radii multiplied by a scale factor 1.20. Additional spheres are computed with the standard parameters of GEPOL.[25]

Applications and Results

While the VBPCM procedure does not consider microscopic effects of solvation, at the molecular level, it is nevertheless a starting point that provides a vivid demonstration of the solvation effect on the solute as such. This is demonstrated by the following examples.

A. Dissociation of LiF. The dissociation of LiF is taken as the first example. It is well known that LiF is a typical ionic compound; it will dissociate to neutral atoms in a vacuum, but in aqueous solution it will give a pair of ions. The dissociation process is studied quantitatively using the VBPCM//VBSCF procedure. VBSCF calculations are performed both in a vacuum and in aqueous solution. Two basis sets, 6-31G* and 6-31+G*, are adopted to check the basis-set dependence. The four inner electrons are frozen at the Hartree−Fock level; thus eight valence electrons are included in the VB calculations. Three VB structures, one covalent and two ionic, are usually involved in the dissociation process. However, since the inverse-ionic structure Li^-F^+ is highly unfavorable, only structures **1** and **2** are included in the calculation and are called henceforth Φ_{cov}(**1**) and Φ_{ion}(**2**), respectively.

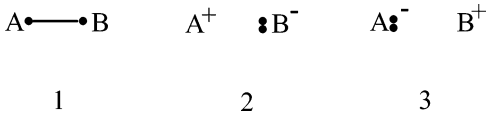

Figures 1 and 2 plot potential-energy curves for the dissociation of LiF with the 6-31G* and 6-31+G* basis sets, respectively. The figures include the ground state (adiabatic profile) and the individual covalent and ionic structures (diabatic profiles). Two main trends in the adiabatic potential are apparent: First, the adiabatic potential-energy curve for the ground state in aqueous solution is stabilized relative to that in a vacuum, by ca. 26 kcal/mol at the equilibrium geometries and ca. 58 kcal/mol at long distances (Figure 1). Second, the solvent affects the geometry of LiF such that the equilibrium bond length is 1.5 Å in a vacuum and 1.6 Å in aqueous solution.

The diabatic profiles tell the classical story of ionic compounds. Thus, as would be expected from an ionic bond, the energy of the ionic structure at equilibrium geometry is much lower than that of covalent structure, both in a vacuum and in solution. However, the dissociation behaves entirely differently; in the gas phase, the bond dissociates to neutral atoms and in solution to ions. Thus, in a vacuum, we see the usual covalent−ionic crossing that dominates ionic bonds in the gas phase.[26,27] On the contrary, in aqueous solution, the energy of the ionic

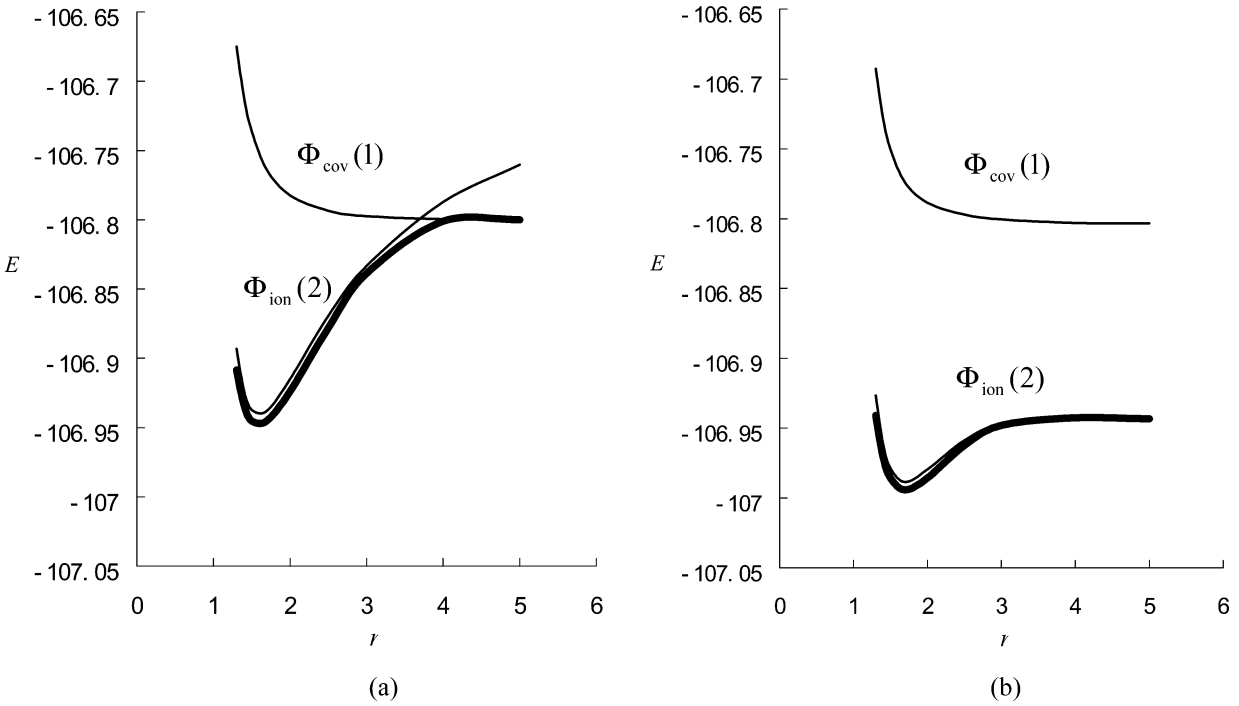

Figure 2. (a) VBSCF/6-31+G* dissociation-energy profiles of LiF in a vacuum. Adiabatic potentials shown in bold curves. (b) VBPCM//VBSCF/6-31+G* dissociation-energy profiles of LiF in H_2O.

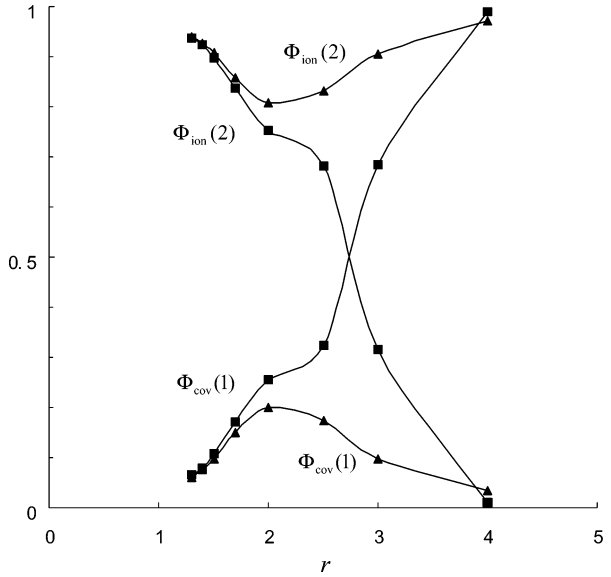

Figure 3. Weights of VB structures of LiF. VBSCF/6-31G* weights are annotated with bold squares and VBPCM//VBSCF/6-31G* weights with triangles.

structure remains quite flat; it rises slightly but does not cross the covalent profile, leading at infinity to two ions, Li^+ and F^-. Thus, the VBPCM calculation shows most lucidly the expected picture, in which the solvent affects significantly the ionic structure, but has almost no effect on the covalent structure. In fact, Figures 1 and 2 reveal the same qualitative behavior and illustrate thereby that the VBPCM method provides *a reasonable physical picture* without much dependence on the basis set.

This qualitative physical picture is further elucidated by looking at the weights of the VB structures along the bond stretch coordinate. Figure 3 shows these weights for the calculations using the 6-31G* basis set. It can be seen that the weights of the two structures at equilibrium distance, in aqueous solution, are virtually identical to those in a vacuum. The weights of the ionic structure both in a vacuum and in solution are ca. 90%, while the weights of the covalent structure are ca. 10%. However, the weight of the covalent structure in a vacuum rises rapidly with the increase of the bond length, while the weight of ionic structure decreases sharply to zero. In solution, the weights of the two structures vary flatly. The weight of ionic structure reaches to 100% at infinity, while the weight of the covalent structure is zero. This is consistent with Figures 1 and 2; the molecule dissociates to Li^+ and F^- in solution and to atoms in a vacuum. Figures 1−3 are in good agreement with Amovilli's results. However, the diabatic profiles in this paper are variational. In other words, the energy profile of each VB structure is optimized individually by the direct VB procedure and is therefore quasivariational.

While the qualitative picture of LiF dissociation is independent of the basis set, what does depend on the basis set is the location of the covalent−ionic crossing in the gas phase and other quantitative aspects. In Figure 1a, the crossing occurs at 2.7 Å, while in Figure 2a, the crossing point shifts to 3.7 Å. Using a simple model[27] based on considerations of ionization potential of Li, electron affinity of F, and the electrostatic energy in the ionic structure (taking a flat covalent curve) leads to an empirically predicted crossing point at a longer distance of >7 Å. Further improvement of the basis set to one that represents the ions better will change the crossing point in the right direction. However, the VBSCF procedure will never really reproduce the empirical result, and one must move on to more sophisticated VB methods, such as BOVB[28] or VBCI.[29] Another quantitative aspect is the solvation energy of the ions, which is around 120 kcal/mol at the longest distance and around 30 kcal/mol at equilibrium position in Figures 1b and 2b. The value at long distance is way too low, since just the solvation energy of Li^+ or of F^- alone is of the order of 100 kcal/mol. Therefore, the PCM method overestimates the ion pairing and predicts a significant barrier (55 kcal/mol for 6-31G* and 30 kcal/mol for 6-31+G*) for ionic dissociation. The bond energy of ion pairs aqueous solution is expected to be less than 5 kcal/mol.[30] Thus,

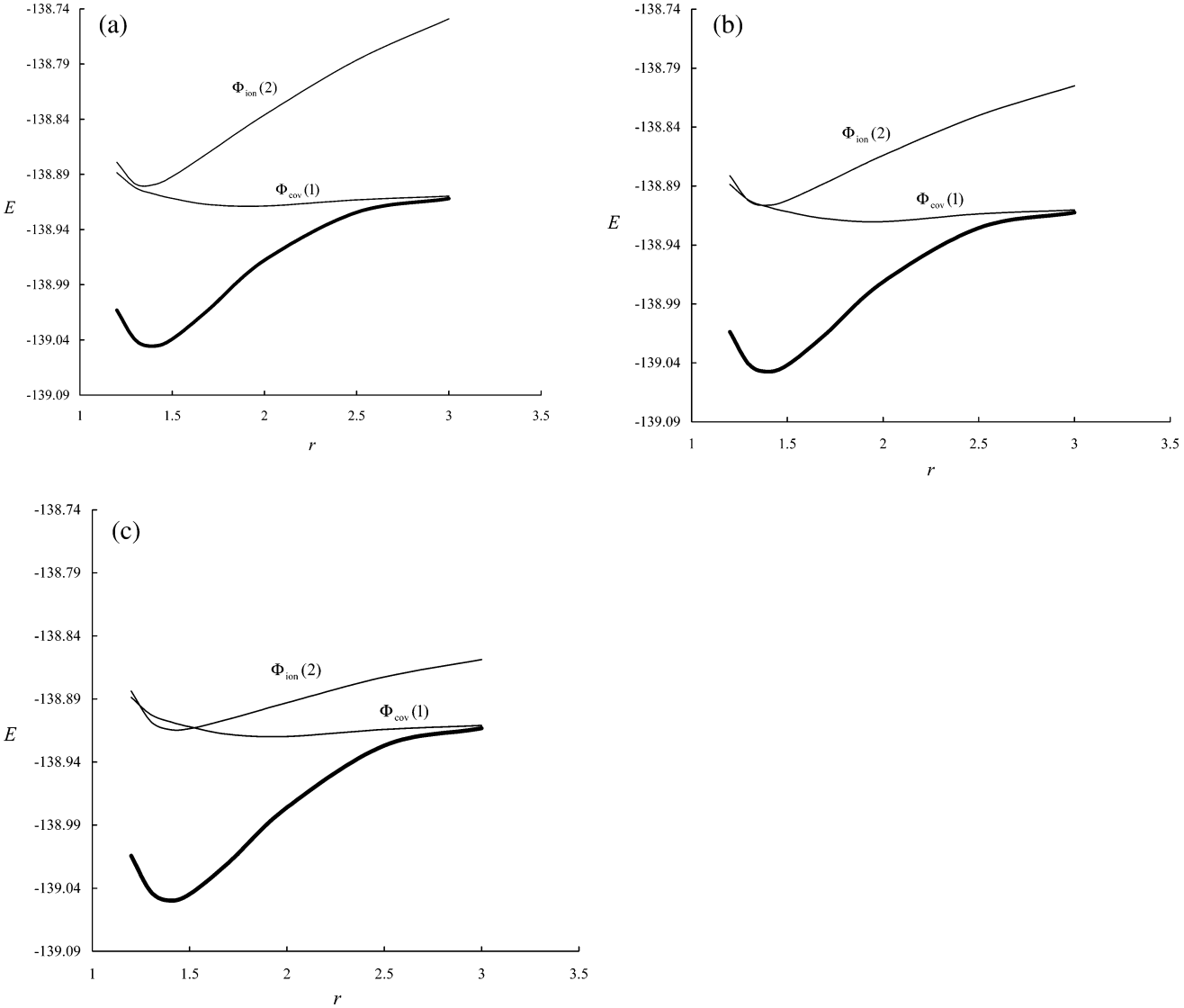

Figure 4. (a) VBSCF/6-31G* dissociation-energy profiles of CH_3F in a vacuum. The adiabatic potential is the bold curve. (b) VBPCM//VBSCF/6-31G* dissociation energy profiles of CH_3F in CCl_4. The adiabatic potential is the bold curve. (c) VBPCM//VBSCF/6-31G* dissociation-energy profiles of CH_3F in H_2O. The adiabatic potential is the bold curve.

with a more refined solvation model, a more sophisticated VB method, and further improvement of the basis, one would expect a flatter ionic curve.

B. Dissociation of Polar-Covalent Bonds. *The C−F Bond in CH_3F.* For bond dissociation of archetypal polar-covalent bonds, we selected two cases. The first one is the C−F bond dissociation in the CH_3F molecule. Two solvents, H_2O and CCl_4, were used to study the dissociation of the molecule, where H_2O is a typical polar solvent while CCl_4 is a nonpolar one. The 6-31G* basis set was applied for the calculation. The 1s electrons of the C and F atoms are frozen at the Hartree−Fock level. Like LiF, here only structures Φ_{cov}(**1**) and Φ_{ion}(**2**) are involved in the calculation.

Figure 4 shows the potential-energy profiles for the dissociation of CH_3F in a vacuum and in solutions. It can be seen that the energies of the covalent structure both in a vacuum and in solutions are virtually identical throughout the profile, while the energies of the ionic structure are significantly different. The ionic structure is stabilized by ca. 9 kcal/mol at equilibrium geometry and the stabilization energy increases, as expected, quickly with increase in the C−F distance. Once again, the solvent is seen to exert significant effect on the ionic structure but not on the covalent one. However, by contrast to the LiF bond, the C−F bond dissociates to radicals, both in a vacuum and in solutions. Furthermore, the covalent structure dominates the wave function throughout the C−F distance. As a result, the adiabatic energy profiles for vacuum and solutions almost overlap and both converge to the energies of the covalent structure at infinity. Another difference with respect to the case of LiF is the significant covalent−ionic resonance energies between the two structures at equilibrium both in a vacuum and in solutions.

To examine solvent effect, Figure 5 shows of the weights of the covalent and ionic structures of the C−F bond in vacuum, CCl_4, and H_2O. The weights of the two structures reflect the fact that the bond is essentially covalent and its adiabatic profiles exhibit small sensitivity to the change of environment. Nevertheless, since the solvent affects the energy of the ionic structure, in proportion to the solvent polarity, the solvent effect in aqueous solution is slightly bigger than that of CCl_4 such that the contributions of the ionic structure follows the trend vacuum $< CCl_4 < H_2O$.

Once again, one must compare the VB picture to a physical picture obtained from empirical considerations. Thus, using the ionization potential of the methyl radical (226.9 kcal/mol) and the electron affinity of fluorine (78 kcal/mol), the covalent−

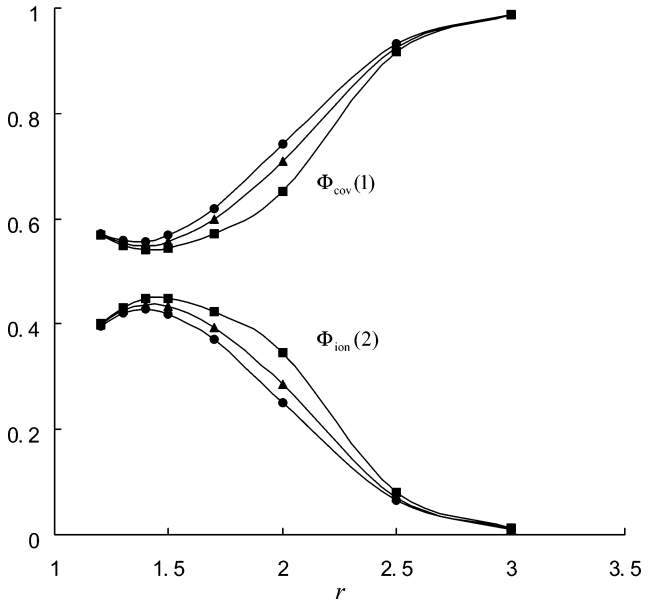

Figure 5. VBSCF/6-31G* and VBPCM//VBSCF/6-31G* weights of VB structures of CH_3F along the C−F dissociation coordinate. The curves in a vacuum, CCl_4, and H_2O are annotated with bold squares, triangles, and circles, respectively.

ionic energy gap at the dissociation limit should reach 149 kcal/mol. Solvation energies of F^- and CH_3^+ are not known, but their combined values is expected to be of the order of this gap, in water, and somewhat less in CCl_4. Clearly, as we already commented, the VBSCF method underestimates the stabilization of the ions at their dissociation limit, and the PCM further underestimate their solvation energies.

Dissociation of the C−Cl Bond in $(CH_3)_3CCl$. The second case of a polar-covalent bond is the C−Cl bond dissociation of tertiary butyl chloride (t-BuCl), which forms a paradigm for the S_N1 mechanism. This reaction has been the target of experimental and theoretical studies.[12b,13,31−33] The 6-31G basis set was used in conjunction with the IEFPCM/UAHF[34] PCM procedure. The inner shell electrons of C and Cl as well as all the π-type doubly occupied orbitals were frozen at their Hartree−Fock levels. Like CH_3F, here only structures Φ_{cov}(**1**) and Φ_{ion}(**2**) were involved in the calculation. Figure 6 shows the potential-energy profiles for the dissociation of t-BuCl in a vacuum and in aqueous solution. It can be seen that the adiabatic potential-energy curve for the ground state in aqueous solution is stabilized relative to that in a vacuum, by ca. 4 and 69 kcal/mol, respectively, at the equilibrium geometry and at a long distance. Also, like the case of LiF, here too, the solvent effect lengthens the C−Cl equilibrium bond length by 0.1 Å. As expected,[11a,12b,13a,28c,35] the dissociation in solution is entirely different from that in the gas phase. In solution, the molecule dissociates to ions, via crossing and avoided crossing of the covalent and ionic structures at C−Cl distance of 2.3 Å, while in the gas phase, the dissociation results in two neutral fragments. This is the classical picture of the first step in the S_N1 mechanism.[35] However, in contrast to the commonly accepted picture,[36] there is not an ion-pair intermediate during the dissociation process. The barrier for the bond dissociation is calculated to be 27.8 kcal/mol, compared with the expected 19.5 kcal/mol.[31] This shows again that a more sophisticated solvent model and higher-level VB treatment will be required in order to study the details of the S_N1 mechanism.

An interesting feature of the energy profile in a vacuum, in Figure 6a, is the double crossing of the covalent and ionic curves at 2.6 and 5.7 Å. This could originate in the fact that VBSCF underestimates the gap between the ionic and covalent structures at infinity. Thus, the VBSCF gap is ca. 56 kcal/mol, while an estimated experimental value, as the difference between the ionization potential of t-Bu· and the electron affinity of Cl, is ca. 84 kcal/mol. If we shift the energy profile of the ionic structure by this difference of ∼30 kcal/mol, the double crossing would vanish, as may be seen in the dashed curve in Figure 6a. However, even now, the covalent and ionic curves are in a touching situation, and therefore, the bond ionicity at a C−Cl bond distance of ca. 3 Å is expected to be significant. Indeed, this high ionicity around 3 Å is reproduced also by the Mulliken charges at the HF and MP2 levels ($Q_{Cl} = -0.82$ and -0.68, respectively). The same type of double crossing was obtained by empirical VB calculations by Hynes.[13a]

C. S_N2 Reaction. The S_N2 reaction is an archetypal process that exhibits a marked-solvent effect[37] and hence was chosen as a target for application of the VBPCM method. The identity reaction $Cl^- + CH_3Cl \rightarrow ClCH_3 + Cl^-$ has been among the most widely studied reaction.[12,37] A Monte Carlo simulation predicted that the activation free energy in solution is increased by 15 kcal/mol over the reaction in the gas phase.[38] The experimentally estimated barrier for this reaction in aqueous solution is 26.6 kcal/mol.[39,40] This reaction was studied with an attempt to see whether VBCPM can reproduce the barrier and whether it can lead to its analysis using the VBSCD model.[41]

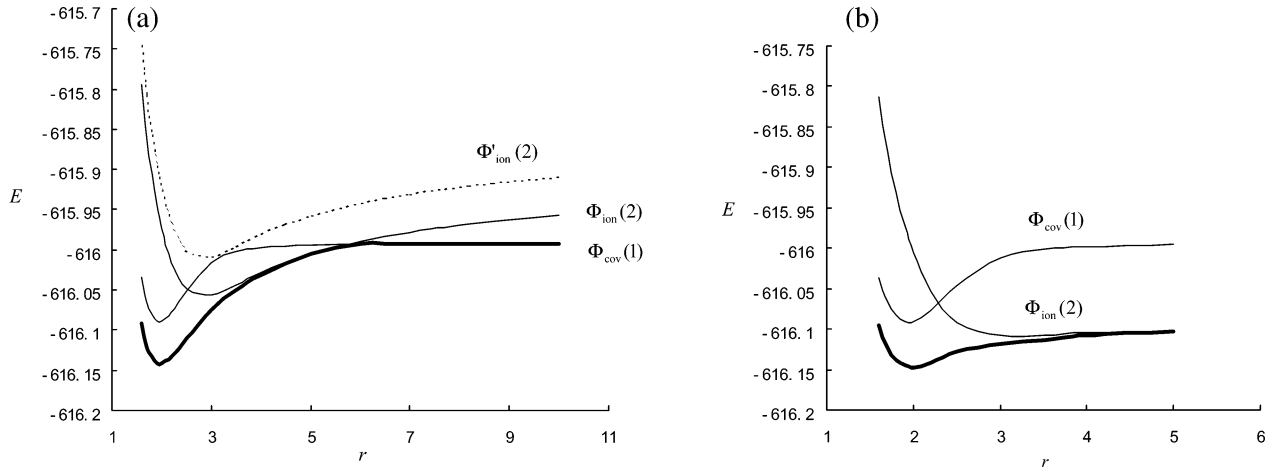

Figure 6. (a) VBSCF/6-31G dissociation energy profiles for $(CH_3)_3CCl$ in a vacuum. The adiabatic potential is shown by the bold curve. Φ'_{ion}(2) is obtained by shifting Φ_{ion}(**2**) by 30 kcal/mol. (b) The VBPCM//VBSCF/6-31G-calculated C−Cl bond dissociation profiles for $(CH_3)_3CCl$ in H_2O. The adiabatic potential is shown by the bold curve.

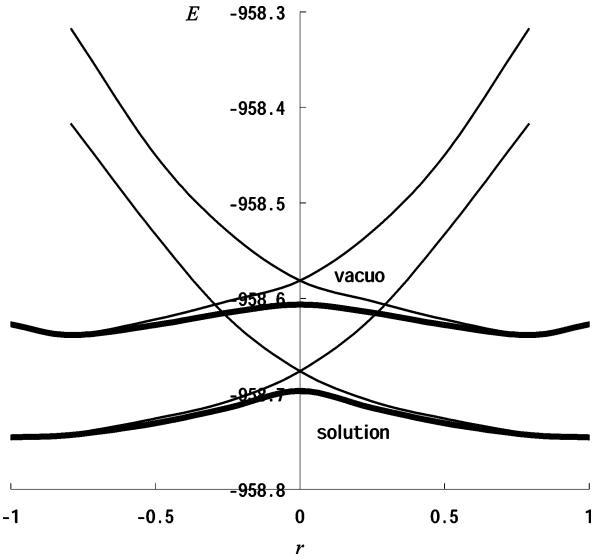

Figure 7. VBPCM//VBSCF/6-31G calculated VBSCD for the identity S_N2 reaction of Cl^- exchange. The Lewis curves are shown by the thin lines and the adiabatic curves by the bold lines.

The 6-31G basis set was applied for this reaction. The inner electrons and π electrons in valence shell were frozen at the Hartree−Fock level, leaving 10 valence electrons to be treated in the VB computation. Structures **4**−**9** describe all the possible ways to distribute the four electrons of the anion Cl^- and the C−Cl bond. Structures **4** and **7** correspond to the covalent Heitler−London structures, which describe the spin pairing in the C−Cl bonds of reactants and products, respectively. Structure **6** is the most stable triple-ion configuration with a positive charge on the central methyl moiety and two negative charges on the chlorines. Structure **9**, known as the "long-bond structure", possesses spin pairing of the odd electrons on the two chlorines and a negative charge on the methyl moiety. The remaining structures **5** and **8**, with a negative charge placed on the methyl moiety, have an unfavorable arrangement of the charges, and are of high energies.

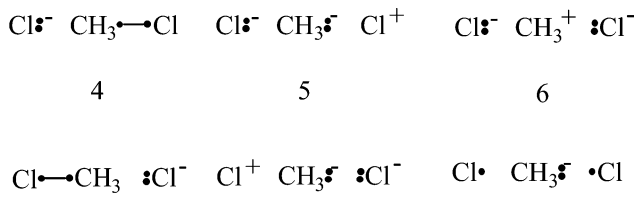

The VBSCD method uses VB theory to provide chemical insight into the barrier and other features of a chemical reaction. The diagram, in Figure 7, is composed of three curves: one is the adiabatic energy profile of the ground state that involves all six structures, and the other two are the reactant and product curves, called also diabatic curves. Structures **4**−**6** contribute to the Lewis structure of the reactant, and structures **6**−**8** construct the Lewis structure of the product. The two Lewis curves cross at the transition state, but the adiabatic state energy is lower than the crossing point of the Lewis curves because of the resonance mixing of two Lewis structures. Table 1 shows the reaction VBSCF calculated barriers and resonance energies for the process in a vacuum and in aqueous solution. It can be seen that the value of the reaction barrier in aqueous solution is 30.5 kcal/mol, which is 3.9 kcal/mol higher than the experimental datum and is 10.6 kcal/mol higher than the corresponding barrier in a vacuum. The resonance energy at the transition state in aqueous solution is ca. 2.9 kcal/mol smaller than that in a vacuum. This illustrates that the solvent affects not only the energies of Lewis structures, but it also changes the interaction between the two Lewis structures. The reduction in the resonance energy follows the VBSCD analysis,[41] which predicts that when the transition state acquires a higher triple-ion character its resonance energy will diminish. Nevertheless, the contribution to the transition-state resonance energy is small and justifies its neglect in qualitative considerations. We should stress once again that the quantitative performance relative to experiment should not be taken as a test of accuracy. It is expected that higher-level ab initio VB methods[28,29] will be required to tackle the quantitative issue.

TABLE 1: VB Properties for the $Cl^- + CH_3Cl \rightarrow ClCH_3 + Cl^-$ (kcal/mol) Reaction

	vacuum	aqueous solution
barrier	19.9	30.5
resonance energy	15.8	12.9

Figure 7 shows the VBSCD for the reaction, where reaction coordinate is defined as the bond order difference

$$Q = n_1(d_1) - n_2(d_2) \qquad n(d) = e^{-a(d-d_0)} \tag{16}$$

where $n(d)$ is determined for any given distance (d) relative to the equilibrium distance (d_0) of Cl−C. The constant a is conveniently chosen so as to make the n value equal 0.5 at the transition state. It can be seen that a minimum occurs at the geometry of the ion−dipole complex for the adiabatic profile in a vacuum, while in a water solution, this minimum is diminished due to the relative strength of the water−chloride ion interaction. This is in agreement with previous studies.[38] The ability to generate the entire VBSCD with diabatic and adiabatic curves is a good feature of the VBPCM method, which will enable us to analyze the factors that determine the barrier height. One feature however is missing, and this is the effect of nonequilibrium solvation. This feature cannot be introduced with the PCM model and would require more sophisticated solvation treatments.

Conclusions

This paper presents a VB method that incorporates the PCM. In VBCPM, the one-electron density plays a role as a bridge between the VB and the PCM methods. In a fashion similar to the MO-based PCM methods, the VBPCM method achieves self-consistency between the charge distribution of the solute and the solvent's reaction field. However, the use of a VB method for the part of quantum mechanics provides added qualitative insights into the solvent effects of chemical problems. Thus, the VBCPM method enables us to compute the energy profile of the full state as well as of individual VB structure and in so doing to reveal the individual effects of solvent on the constituents of the wave function.

Test calculations, using the VBSCF procedure (hence, VBPCM//VBSCF) for ionic and covalent bond-dissociation processes and for the S_N2 reaction of the chloride exchange show the utility of the VBCPM method. At this point, the method has a qualitative value, but its quantitative aspects are still lacking in two respects. One is the use of VBSCF, which is the basic ab initio VB level available, and better ones exists.[28,29] The second aspect is the continuum solvent model that lacks both discrete description of solvation as well as nonequilibrium effects. These two aspects will have to improve

in the future by upgrading either the VB method, the solvent model, or both. In this respect, we point out that the IEF-PCM model is adopted in the paper for simplicity, but any other modified and improved PCM method may be used in a similar fashion. Furthermore, an alternative and maybe more suitable way to describe solvent effects for diabatic profiles is to apply the nonequilibrium solvation model.[13] This aspect of work is in progress.

Acknowledgment. The research at XMU is supported by the Natural Science Foundation of China (Nos. 20225311, 20373052, and 20021002,) and the TRAPOYT of Ministry of Education of China. The research at Hebrew Uuniversity is supported in part by an Israel Science Foundation grant to S.S.

References and Notes

(1) Reichardt, C. *Solvents and Solvent Effects in Organic Chemistry*, 2nd ed.; VCH: Weihein, 1990.

(2) Rivail, J. L.; Rinaldi, D.; Ruiz-Lopez, M. F. *Liquid-State Quantum Chemistry in Computational Chemistry: Review of Current Trends*; Leszczynski, J., Ed.; World Scientific: Singapore, 1995; p 65.

(3) Cramer, C. J.; Truhlar, D. G. *Solvent Effects and Chemical Reactivity*; Tapia, O., Bertra'n, J., Ed.; Kluwer: Dordrecht, 1996; p 1.

(4) Adamo, C.; Cossi, M.; Rega, N.; Barone, V. In *Theoretical Biochemistry: Processes and Properties of Biological Systems*, Erikson, L. A., Ed.; Elsevier Science: Amsterdam, 2001; p 467.

(5) Tomasi, J.; Persico, M. *Chem. Rev.* **1994**, *94*, 2027.

(6) Cramer, C. J.; Truhlar, D. G. *Chem. Rev.* **1999**, *99*, 2161.

(7) (a) Li, J.; Zhu, T.; Cramer, C. J.; Truhlar, D. G. *J. Phys. Chem. A* **2000**, *104*, 2178. (b) Dolney, D. M.; Hawkins, G. D.; Winget, P.; Liotard, D. A.; Cramer, C. J.; Truhlar, D. G. *J. Comput. Chem.* **2000**, *21*, 340.

(8) Orozco, M.; Luque, F. J. *Chem. Rev.* **2000**, *100*, 4187.

(9) Curutchet, C.; Cramer, C. J.; Truhlar, D. G.; Ruiz-López, M. F.; Rinaldi, D.; Orozco, M.; Luque, F. J. *J. Comput. Chem.* **2003**, *24*, 284.

(10) See, for example, a few methods described in: *Valence Bond Theory*; Cooper, D. L., Ed.; Elsevier Science: Amsterdam, 2002.

(11) (a) Warshel, A.; Weiss, R. M. *J. Am. Chem. Soc.* **1980**, *102*, 6218. (b) Qvist, J.; Warshel, A. *Chem. Rev.* **1993**, *93*, 2523.

(12) (a) Shaik, S. *J. Am. Chem. Soc.* **1984**, *106*, 1227. (b) Shaik, S. *J. Org. Chem.* **1987**, *52*, 1563. (c) Shaik, S. *Prog. Phys. Org. Chem.* **1985**, *15*, 197.

(13) (a) Kim, H. J.; Hynes, J. T. *J. Am. Chem. Soc.* **1992**, *114*, 10508. (b) Mathias, J. R.; Bianco, R.; Hynes, J. T. *J. Mol. Liq.* **1994**, *61*, 81. (c) Timoneda, J. I.; Hynes, J. T. *J. Phys. Chem.* **1991**, *95*, 10431. (d) Kim, H. J.; Hynes, J. T. *J. Chem. Phys.* **1992**, *96*, 5088.

(14) (a) Amovilli, C.; Mennucci, B. *J. Phys. Chem. B* **1997**, *101*, 1051. (b) Amovilli, C.; Mennucci, B.; Floris, F. M. *J. Phys. Chem. B* **1998**, *102*, 3023. (c) Amovilli, C.; Barone, V.; Cammi, R.; Cances, E.; Cossi, M.; Mennucci, B.; Pomelli, C.; Tomasi, J. *Adv. Quantum Chem.* **1999**, *32*, 227.

(15) Mo, Y.; Gao, J. *J. Comput. Chem.* **2000**, *21*, 1458.

(16) (a) Miertus, S.; Scrocco, E.; Tomasi, J. *Chem. Phys.* **1981**, *55*, 117. (b) Tomasi, J.; Persico, M. *Chem. Rev.* **1994**, *94*, 2027. (c) Cammi, R.; Tomasi, J. *J. Comput. Chem.* **1995**, *16*, 1449.

(17) McWeeny, R. *Int. J. Quantum Chem.* **1988**, *34*, 25.

(18) (a) Zhang, Q.; Li, X. *THEOCHEM* **1989**, *189*, 413. (b) Wu, W.; Mo, Y.; Zhang, Q. *THEOCHEM* **1993**, *283*, 227. (c) Wu, W.; Mo, Y.; Cao, Z.; Zhang, Q. *Valence Bond Theory*; Cooper, D. L., Ed.; Elsevier Science: Amsterdam, 2002; p 143.

(19) Chirgwin, H. B.; Coulson, C. A. *Proc. R. Soc. London, Ser. A* **1950**, *2*, 196.

(20) Cancès, E.; Mennucci, B.; Tomasi, J. *J. Chem. Phys.* **1997**, *107*, 3032.

(21) (a) Verbeek, J.; van Lenthe. J. H. *THEOCHEM* **1991**, *229*, 115. (b) van Lenthe, J. H. *Int. J. Quantum Chem.* **1991**, *40*, 201. (c) Balint-Kurti, G. G.; Benneyworth, P. R.; Davis, M. J.; Williams, I. H. *J. Phys. Chem.* **1992**, *96*, 4346.

(22) Schmidt, M. W.; Baldridge, K. K.; Boatz, J. A.; Elbert, S. T.; Gordon, M. S.; Jensen, J. J.; Koseki, S.; Matsunaga, N.; Nguyen, K. A.; Su, S.; Windus, T. L.; Dupuis, M.; Montgomery, J. A. GAMESS. *J. Comput. Chem.* **1993**, *14*, 1347.

(23) Song, L.; Wu, W.; Mo, Y.; Zhang, Q. *XMVB: An Ab Initio Nonorthogonal Valence Bond Program*; Xiamen University: Xiamen, 1999.

(24) (a) Cances, M. T.; Mennucci, V.; Tomasi, J. *J. Chem. Phys.* **1997**, *107*, 3032. (b) Cossi, M.; Barone, V.; Mennucci, B.; Tomasi, J. *Chem. Phys. Lett.* **1998**, *286*, 253.

(25) Pascual-Ahuir, J. L.; Silla, E.; Tomasi, J.; Bonaccorsi, R. *J. Comput. Chem.* **1987**, *8*, 778.

(26) (a) Herzberg, G. *Diatomic Molecules*, 2nd ed.; Van Nostrand: Princeton, NJ, 1950; pp 372. (b) Salem, L. *Electrons in Chemical Reactions: First Principles*; Wiley: New York, 1982.

(27) Kauzmann, W. *Quantum Chemistry*; Academic Press: New York, NY, 1957; pp 536−538.

(28) (a) Hiberty, P. C.; Flament, J. P.; Noizet, E. *Chem. Phys. Lett.* **1992**, *189*, 259. (b) Hiberty, P. C.; Humbel, S.; Byrman, C. P.; Van Lenthe, J. H. *J. Chem. Phys.* **1994**, *101*, 5969. (c) Hiberty, P. C.; Shaik, S. *Theor. Chem. Acc.* **2002**, *108*, 255.

(29) (a) Wu, W.; Song, L.; Cao, Z.; Zhang, Q.; Shaik, S. *J. Phys. Chem. A* **2002**, *105*, 2721. (b) Song, L.; Wu, W.; Zhang, Q.; Shaik, S. *J. Comput. Chem.* **2004**, *25*, 472.

(30) (a) Karim, O. A.; McCammon, J. A. *J. Am. Chem. Soc.* **1986**, *108*, 1762. (b) Jorgensen, W. L.; Buckner, J. K.; Huston, S. E.; Rossky, P. J. *J. Am. Chem. Soc.* **1987**, *109*, 1891.

(31) Jorgensen, W. L.; Buchner, J. K.; Huston, S. E.; Rossky, P. J. *J. Am. Chem. Soc.* **1987**, *109*, 1891.

(32) Hartsough, D. S.; Merz, K. M., Jr. *J. Phys. Chem.* **1995**, *99*, 384.

(33) Yamabe, S.; Tsuchida, N. *J. Comput. Chem.* **2004**, *25*, 598.

(34) Barone, V.; Cossi, M.; Mennucci, B.; Tomasi, J. *J. Chem. Phys.* **1997**, *107*, 3210.

(35) Pross, A.; Shaik, S. *Acc. Chem. Res.* **1983**, *16*, 363.

(36) For example, Lowry, T.; Richardon, K. S. *Mechanism and Theory in Organic Chemistry*; Harper and Row: New York, 1995.

(37) Shaik, S.; Schlegel, H. B.; Wolfe, S. *Theoretical Aspects of Physical Organic Chemistry*; Wiley-Interscience: New York, 1992.

(38) (a) Chandrasekhar, J.; Smith, S. F.; Jorgensen, W. L. *J. Am. Chem. Soc.* **1984**, *106*, 3049. (b) Chandrasekhar, J.; Jorgensen, W. L. *J. Am. Chem. Soc.* **1985**, *107*, 2975. (c) Mathis, J. R.; Bianco, R.; Hynes, J. T. *J. Mol. Liq.* **1994**, *61*, 81.

(39) Cox, G. B.; Hedwig, G. R.; Parker, A. J.; Watts, D. W. *Aust. J. Chem.* **1974**, *27*, 477.

(40) Abraham, M. H. *J. Chem. Soc., Perkin Trans. 2* **1976**, 1375.

(41) Shaik, S.; Shurki, A. *Angew. Chem.* **1999**, *38*, 586.